ATMOSPHERIC SCIENCE LETTERS
Atmos. Sci. Let. **17**: 415–421 (2016)
Published online 16 June 2016 in Wiley Online Library
(wileyonlinelibrary.com) **DOI:** 10.1002/asl.673

RMetS
Royal Meteorological Society

Hurricane simulation using different representations of atmosphere–ocean interaction: the case of Irene (2011)

P. A. Mooney,[1]* D. O. Gill,[1] F. J. Mulligan[2] and C. L. Bruyère[1]

[1]*Mesoscale and Microscale Meteorology Laboratory, National Center for Atmospheric Research (NCAR), Boulder, CO, USA*
[2]*Department of Experimental Physics, Maynooth University, Kildare, Ireland*

**Correspondence to:*
P. A. Mooney, Mesoscale and Microscale Meteorology Laboratory, National Center for Atmospheric Research, P.O. Box 3000, Boulder, CO 80307-3000, USA.
E-mail: pmooney@ucar.edu

Received: 11 March 2016
Revised: 12 May 2016
Accepted: 25 May 2016

Abstract

Three approaches to represent sea surface temperatures (SSTs) in atmospheric models have been investigated using the Weather Research and Forecasting model: (1) prescribing SSTs every 6 h from reanalysis, (2) a one-dimensional ocean mixed-layer model and (3) a fully coupled regional ocean model. Hurricane Irene (2011) was chosen as the test case. All three options produced results comparable to observations immediately after storm passage but only options (1) and (3) captured recovery to pre-storm conditions which suggests both are feasible approaches for long-term simulations of tropical cyclones. Option (2) merits further investigation because of its greater computational efficiency and reduced complexity.

Keywords: Weather Research and Forecasting (WRF) model; sea surface temperatures; ocean mixed-layer model; coupled atmosphere–ocean model; WRF–ROMS; hurricanes

1. Introduction

Sea surface temperature plays an important role in the life cycle of a tropical cyclone (TC) and is one of the main factors for cyclogenesis (e.g. Bruyère *et al.*, 2012). As a TC passes over the warm ocean surface, it reduces the temperature of the sea surface leaving a cold wake that continues to cool for up to 2 days afterwards and may extend for hundreds of kilometres adjacent to the storm track (Dare and McBride, 2011). The magnitude of this cooling can be up to 9 °C as shown by Lin *et al.* (2003) for the case of Kai-Tak (2000) in the South China Sea. This cooling depends strongly on the TC intensity, its translational speed and the depth of the ocean mixed layer (Dare and McBride, 2011).

The time required for SSTs to return to their climatological values varies widely between TCs with recovery periods ranging from 1 to 60 days (Hart *et al.*, 2007) with the majority recovering within 30 days after a TC has passed (Dare and McBride, 2011). These lingering cold wakes can impact seasonal TC activity as later storms may interact with them; the probability for cyclones to encounter a cold wake is ~10% on average (Balaguru *et al.*, 2014). This additional mixing may also be important on longer time scales through its impact on the large-scale slowly varying ocean overturning circulation, and may impact the long-term climatology of TCs (Dare and McBride, 2011). Clearly, it is important to include the ocean response to hurricanes in atmospheric models used for long-term studies of TCs. Since most atmospheric models represent the oceanic response solely through changes in SSTs, it is essential to accurately represent them in models.

When the focus of hurricane studies moves from weather forecasting to regional climate studies, computational efficiency becomes increasingly important and the benefits of more realistic representations of physical processes in the model must be critically assessed. This study examines three different methods of representing SSTs in the Weather Research and Forecasting (WRF) model to determine the impact of trading computational efficiency for model configuration, to inform the representation of SSTs in atmospheric models for long-term studies of TCs. Hurricane Irene (2011) was chosen as a case study because most forecast models failed to correctly predict the cyclone intensity due to underestimated storm-induced upper-ocean cooling (Glenn *et al.*, 2016). Simulations are evaluated against the best track, satellite and buoy data.

2. Model domains and details

2.1. The Weather Research and Forecasting (WRF) model

All simulations use the WRF model (Skamarock *et al.*, 2008) over the two domains shown in Figure 1 with two-way nesting, 51 model levels and a model top at 10 hPa. The outer domain in Figure 1 has a grid spacing of 36 km with 340 × 260 (east–west × north–south) grid points, while the inner domain has a 12-km spacing with 802 × 511 grid points. Each simulation covers the 14-day period beginning at 0000 UTC on the 23 August 2011 with initial conditions and 6-h boundary conditions derived from ERA-Interim (Dee *et al.*, 2011).

The WRF parameterization schemes used are the Community Atmosphere Model (Collins *et al.*, 2004)

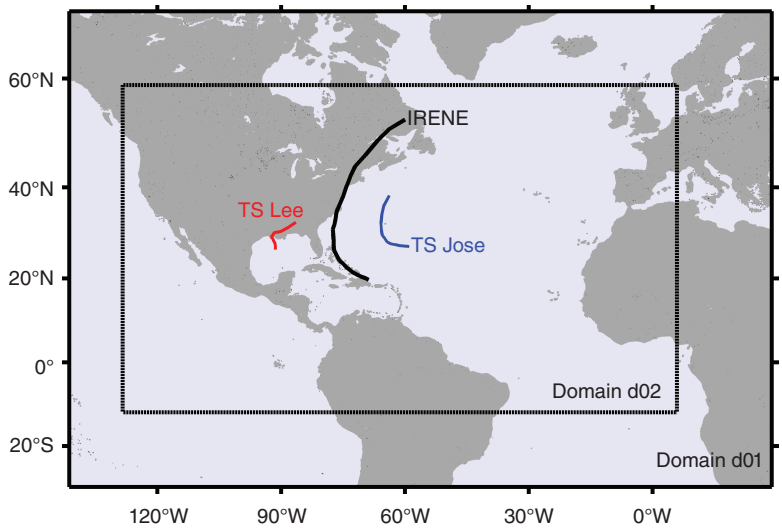

Figure 1. Outer 36-km WRF domain d01 and inner 12-km WRF domain d02. Also shown are the tracks of hurricanes Irene (23 August 2011 to 30 August 2011) and Tropical Storms (TS) Lee (2 September 2011 to 6 September 2011) and Jose (26 August 2011 to 29 August 2011).

longwave and shortwave radiation schemes, the Kain-Fritsch cumulus scheme (Kain and Fritsch, 1990; Kain, 2004), the Yonsei University planetary boundary layer scheme (Hong *et al.*, 2006), the WRF single moment six-class scheme (Hong and Lim, 2006) and the Noah land surface model (Chen and Dudhia, 2001). Analysis of 16 WRF simulations using different combinations of physical parameterization schemes has shown that this combination accurately simulates the track and minimum pressures of Irene (not shown). Three different approaches of updating SSTs are used with this WRF configuration (see Table 1) to simulate the passage of Irene.

2.2. Representation of the ocean surface

2.2.1. ERA-Interim SSTs

In this simulation, WRF uses daily averaged SSTs from ERA-Interim, which are derived from the Operational Sea Surface Temperature and Sea Ice Analysis (OSTIA; Stark *et al.*, 2007). WRF uses the scheme described in Zeng and Beljaars (2005) to modify these daily averages in response to surface winds and changes in the radiative fluxes (e.g. diurnal variations in shortwave radiation).

2.2.2. One-dimensional (1-D) ocean mixed-layer (OML) model

This is a simple 1-D OML model (Davis *et al.*, 2008) based on Pollard *et al.* (1972). Neither horizontal advection nor the pressure gradient are accounted for in this model which simply requires specification of the initial mixed-layer depth (climatological values obtained from www.ifremer.fr/cerweb/deboyer/mld; de Boyer Montégut *et al.*, 2004), the deep layer temperature lapse rate (default 0.14 K/m) and the wind stress at the ocean surface which is provided by the WRF model.

2.2.3. Regional Ocean Modelling System (ROMS)

ROMS (Shchepetkin and McWilliams, 2005) is a three-dimensional (3-D) regional ocean model with terrain following coordinates that solves the free surface, hydrostatic, primitive equations. In this simulation, ROMS is configured using a single domain which covers the same area as the outer WRF domain. The ROMS domain uses a grid spacing of 12 km and 30 stretched vertical levels. Values for the initial conditions and open boundaries are generated from the global HYbrid Coordinate Ocean Model with Naval Research Lab Coupled Ocean Data Assimilation (HYCOM/NCODA; http://tds.hycom.org/thredds/dodsC/GLBa0.08/expt_90.9; Cummings, 2005).

A 10-day spin-up period is used for ROMS and HYCOM/NCODA tracer and velocity fields are provided using Orlanski-type radiation conditions in conjunction with relaxation. The Flather method was used to obtain boundary values for the free-surface and depth-averaged velocity from HYCOM/NCODA. The Generic Length Scale vertical mixing scheme (Warner *et al.*, 2005) was used to calculate the vertical turbulent mixing and specify the quadratic drag formulation for the bottom friction. Other parameters for ROMS are shown in Table 2.

The coupled WRF–ROMS modelling system used in this study is the Coupled Ocean–atmosphere–Wave–Sediment Transport (Warner *et al.*, 2010) modelling system. These models exchange data once per hour: WRF receives SSTs from ROMS every hour while providing ROMS with wind stress, sea level pressure and surface heat fluxes.

2.3. Data sets

ERA-Interim was obtained on a global 0.75° grid from the European Centre for Medium Range Weather Forecasting data server: http://data.ecmwf.int/data.

Table 1. Summary of the ocean surface representation in each of the WRF simulations.

WRF–ERAI	WRF with updated daily averaged SSTs from ERA-Interim; a diurnal cycle is imposed on the input SST data.
WRF–OML	WRF run with a simple 1-D ocean mixed layer model
WRF–ROMS	WRF fully coupled to a 3-D hydrostatic, primitive equation regional ocean model system (ROMS).

Table 2. Model parameters used in ROMS.

L	1015	Number of I-direction interior rho-points
M	775	Number of J-direction interior rho-points
h_{max}	5000 m	Maximum depth of computational domain
h_{min}	50 m	Minimum depth of computational domain
θ_s	5	Sigma coordinate stretching factor
θ_b	0.4	Sigma coordinate bottom stretching factor
dt (*baroclinic*)	30 s	Baroclinic time step
dt (*barotropic*)	1 s	Barotropic time step
Outflow	10 days	
Inflow	0.5 days	

The OSTIA is provided by GHRSST, UKMO and MyOcean and obtained from http://podaac.jpl.nasa.gov/dataset/UKMO-L4HRfnd-GLOB-OSTIA. This is a Level 4 SST analysis produced daily on a global 0.054° grid by the UK Met Office using optimal interpolation. Best track data for observed hurricanes (Figure 1) were obtained from the International Best Track Archive for Climate Stewardship (Knapp *et al.*, 2010). Buoy data (locations shown in Figure 2) were obtained from the US National Data Buoy Center: http://www.ndbc.noaa.gov/to_station.shtml.

3. Results

Figure 2 shows the difference between pre-storm SSTs (23 August 2011) and post-storm SSTs (27 August 2011; 1 September 2011; 5 September 2011) for the OSTIA satellite data (row one) and the three simulations. This sequence of SST differences shows the cooling generated by Irene and the recovery to pre-storm conditions. Figure 2(a) shows that Irene's passage caused SST cooling of approximately 2–3 °C by the 27 August 2011, while the observed recovery to pre-storm conditions is shown in Figure 2(b) and (c). A wide wake with greater cooling on the right side of the track is clearly evident.

Corresponding results from WRF–ERAI (Figure 2(d)–(f)) are in excellent agreement with the OSTIA results. Small differences arise from the imposed diurnal cycle (described above) and the interpolation of OSTIA's SSTs (12 km) to the coarser ERA-Interim grid (~80 km). Figure 2(e) shows that WRF–ERAI SSTs have begun recovery to pre-storm conditions five days after the passage of Irene. Four days later, the SSTs have almost returned to pre-storm conditions (Figure 2(f)).

The behaviour of SSTs in the WRF–OML simulation is shown in Figure 2(g)–(i). Irene's passage generates a slightly colder wake than observations. Of interest to this study is the absence of a recovery to pre-storm conditions. The cold wake in the WRF–OML simulation shows almost no deterioration even after nine days. Recovery to pre-storm conditions is primarily driven by surface fluxes and horizontal advection (Vincent *et al.*, 2012) which is not represented in the OML model. The WRF–OML has two additional cold wakes associated with tropical storms Jose and Lee shown in Figure 1. Lee is also present in OSTIA (Figure 2(c)), WRF–ERAI (Figure 2(f)) and WRF–ROMS (Figure 2(k)–(l)).

The characteristics of Irene's cold wake in the WRF–ROMS simulation are similar to those observed in the satellite SSTs – wide with greater cooling on the right side of the track. Similar to the WRF–ERAI simulation and satellite SSTs, the cold wake in WRF–ROMS shows some recovery after five days with SSTs partially returning to pre-storm conditions after nine days. However, the WRF–ROMS simulation generates a colder wake than both WRF–ERAI and OSTIA.

This is also evident in Figure 3 which shows the mean SSTs over a square area, whose width is four times the radius of maximum winds and centred on the location of maximum cyclone intensity for each simulation (see Figure 2). The evolution of the SSTs in Figure 3 shows the rapid cooling as Irene passes and the subsequent recovery or the absence of a recovery in the case of WRF–OML. SSTs in WRF–ROMS and WRF–OML show very similar initial cooling, and both show greater cooling than either WRF–ERAI or OSTIA.

While the lower SSTs in WRF–ROMS and WRF–OML may be caused by a slower than observed translational speed, it must be noted that satellite SST measurements are based on a very thin layer of the ocean surface while simulated SSTs can represent a layer several centimetres deep (Costa *et al.*, 2012). For this reason, the simulated SSTs are also compared to measurements from the three buoys (m44014, m44065 and m44013) shown in Figure 2.

A comparison of simulated and observed SSTs, 10-m wind speeds and mean sea level pressure (MSLP) at each buoy is shown in Figure 4. At buoy m44014, the WRF–ERAI simulation shows greater cooling than the other simulations (Figure 4(a)) but it still fails to reach the cold SSTs observed at the buoy. Both WRF–ERAI and WRF–ROMS SSTs show a slow recovery to pre-storm conditions which agrees with the observed rate of warming at the buoy. WRF–ROMS and WRF–OML temperatures show little initial cooling (approximately 1 °C) with no return to pre-storm conditions in the case of WRF–OML. At buoy m44065, SSTs cool by approximately 4 °C as the hurricane passes and continue to cool at a much slower rate for the next day

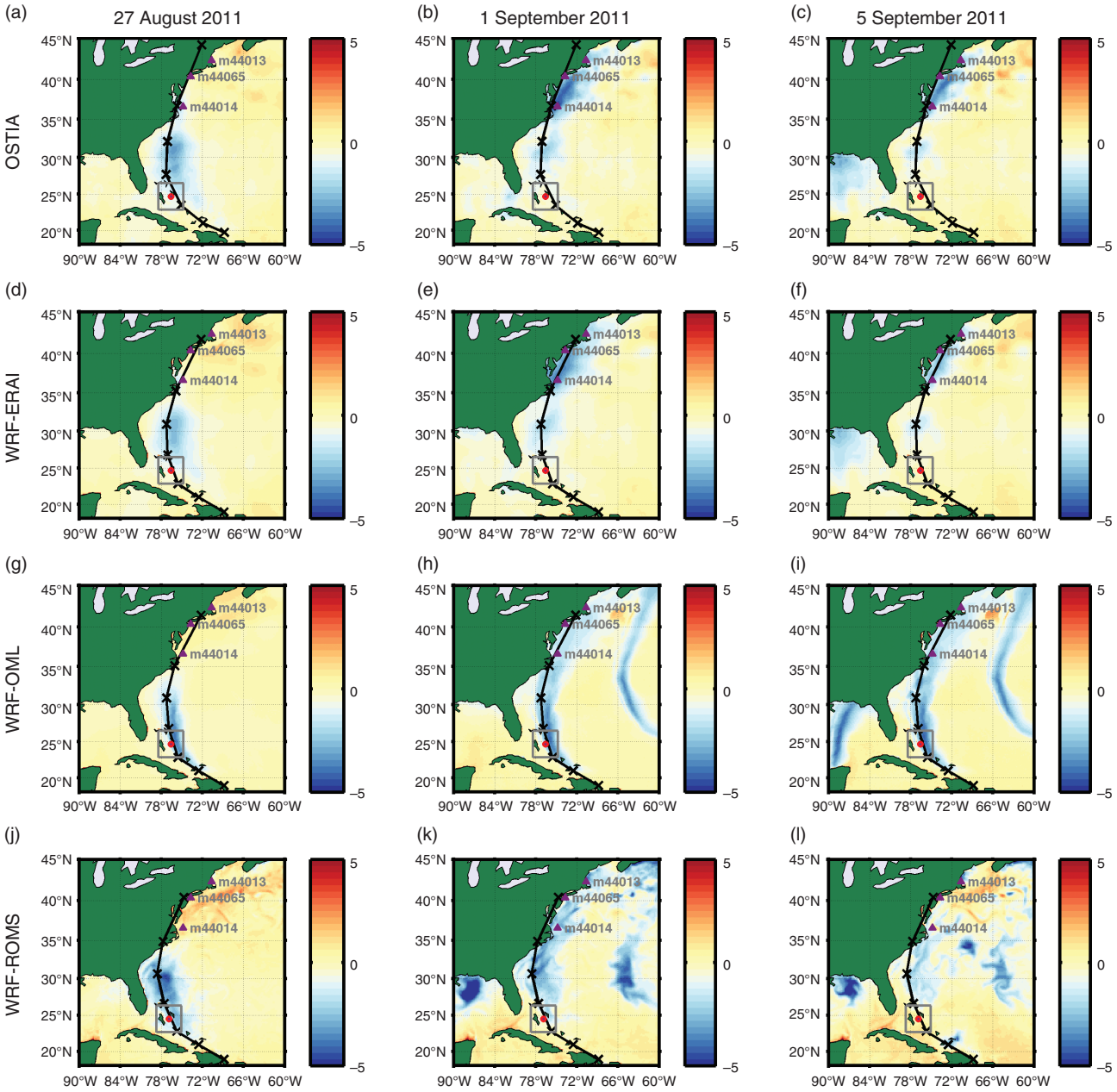

Figure 2. Post-storm cooling in OSTIA sea surface temperatures (a) difference between the 27 August 2011 and the 23 August 2011, (b) difference between the 1 September 2011 and the 23 August 2011, (c) difference between the 4 September 2011 and the 23 August 2011. (d)–(f) Same as (a)–(c) except for WRF–ERAI. (g)–(i) Same as (a)–(c) except for WRF–OML. (j)–(l) Same as (a)–(c) except for WRF–ROMS. SSTs in the square box centred on the red dots are averaged at each time step and the results are displayed in Figure 3.

or so (see Figure 4(b)). This is followed by rapid warming which quickly reduces to a rate of approximately 0.25 °C/day. A week after Irene passed, SSTs at buoy m44065 are still 2 °C colder than pre-storm temperatures. WRF–ERAI SSTs display most of this observed behaviour with the exception of the rapid warming immediately following the passage of Irene. Although WRF–ROMS does simulate the correct temperature three days after the hurricane passed, its SSTs do not show the observed 4 °C drop in temperature immediately following Irene's passage nor the rapid warming subsequent to it. WRF–OML shows cooling that is intermediate between WRF–ERAI and WRF–ROMS but again shows no evidence of recovery to pre-storm conditions.

Although the SSTs at buoy m44013 experience greater cooling (almost 8 °C) than buoy m44065, they behave in a similar way – rapid cooling, followed by a brief period of rapid warming and then a slow oscillatory recovery. This behaviour is well captured by WRF–ROMS that outperforms the other simulations at this buoy, and shows almost 6 °C of cooling. WRF–ERAI SSTs show a similar rate of recovery in the week following Irene's passage, however, it shows only 2 °C of cooling as the hurricane passes and no rapid recovery. The WRF–OML shows very

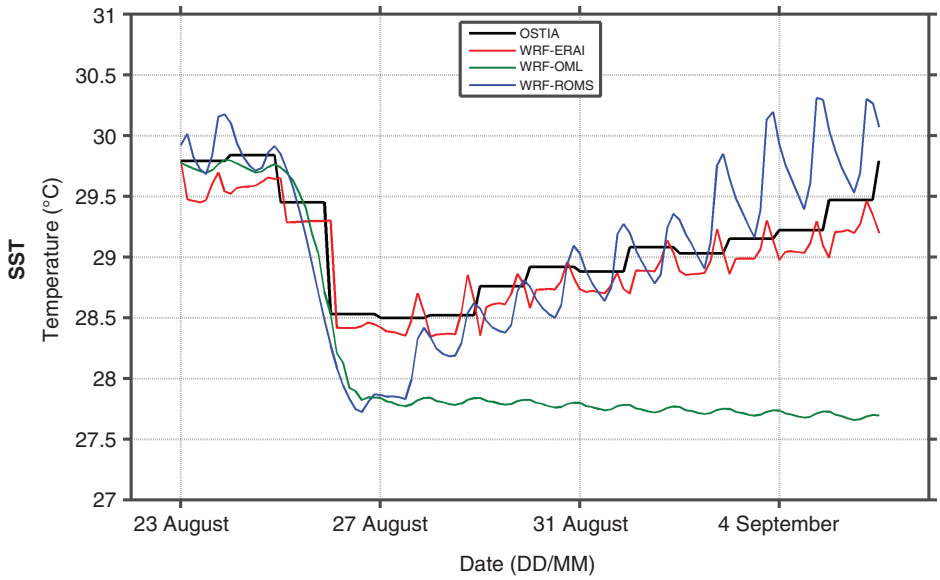

Figure 3. Sea surface temperatures from each simulation and OSTIA averaged over a square box whose width is four times the radius of maximum winds at maximum storm intensity (~4 × 90 km) centred on the location where the hurricane reaches maximum intensity (see red dot near 25°N on Figures 2(a), (d), (g) and (j)).

little cooling (approximately 1 °C) as the hurricane passes.

Figure 4(d)–(f) and Figure 4(g)–(i) show the measured and simulated 10-m wind speeds and MSLP at each buoy. The MSLPs from WRF–ERAI and WRF–OML are in good agreement with those measured at the buoy, except the simulated minimum occurs slightly later than the observed minimum. This is due to the slower than observed translational speed of the simulated cyclones. Similarly, WRF–ROMS shows a delay in the timing of the minimum pressure, which is also 10–15 hPa weaker than the minimum measured at the buoys.

Table 3 shows the root mean squared error (RMSE) of each simulated track (determined from the location of minimum pressure) from the best-observed track. Somewhat surprisingly WRF–ROMS has the greatest departure from the best-observed track. This is partially due to the slower translational speed of the WRF–ROMS simulation.

RMSEs for minimum sea level pressures are also included in Table 3. Clearly the hurricane intensity is well captured by all three simulations, which is in good agreement with the behaviour in pressure noted earlier at the buoys.

4. Discussion and Conclusions

The processes that cause cooling of the upper ocean mixed layer can be divided into those that are responsible for cooling the ocean surface within hours of the TC arrival and those that continue the cooling for up to two days after the TC has passed (Hart *et al.*, 2007). The dominant mechanisms for cooling the ocean surface are transient upwelling and wind-driven oceanic turbulence that causes vertical mixing and entrainment of colder water from below the thermocline into the overlying mixed layer (Vincent *et al.*, 2012). Other processes include enhanced surface sensible and latent heat fluxes from the ocean to the atmosphere driven primarily by the winds near the radius of maximum wind (Price, 1981), horizontal transport of warm water away from the storm centre (Leipper, 1967), precipitation falling into the ocean surface and radiative losses (Brand, 1971). Those processes which cool the sea surface temperature in the vicinity of the storm have the greatest impact as they reduce the amount of heat and moisture available to the tropical storm which in turn limits its intensity (Yablonsky *et al.*, 2015). In addition to influencing the individual TC, the cold wake may also impact other storms that interact with it at a later stage (Balaguru *et al.*, 2014).

In WRF, the coupled ocean model (WRF–ROMS) is the most physically realistic simulation of the air–sea interaction and it produces SSTs similar to observed values, but it is computationally expensive. For example, WRF–ROMS used 1.5 times as many processors and 60% more computational time than WRF–ERAI.

The WFR–ERAI is a good, less-expensive alternative to WRF–ROMS and as a result it continues to be in widespread use by the regional climate modelling community. However, it cannot represent the feedback between the atmosphere and ocean. This could have implications for long-term climate simulations of TCs, where TCs in regional models do not coincide with TC tracks in SSTs from the parent model. This can impact TC genesis, track and intensity in regional climate simulations.

WRF with the one-dimensional ocean mixed-layer model (WRF–OML) is capable of simulating the cold wake in the SSTs caused by the passage of hurricane Irene which makes it useful for short-term studies.

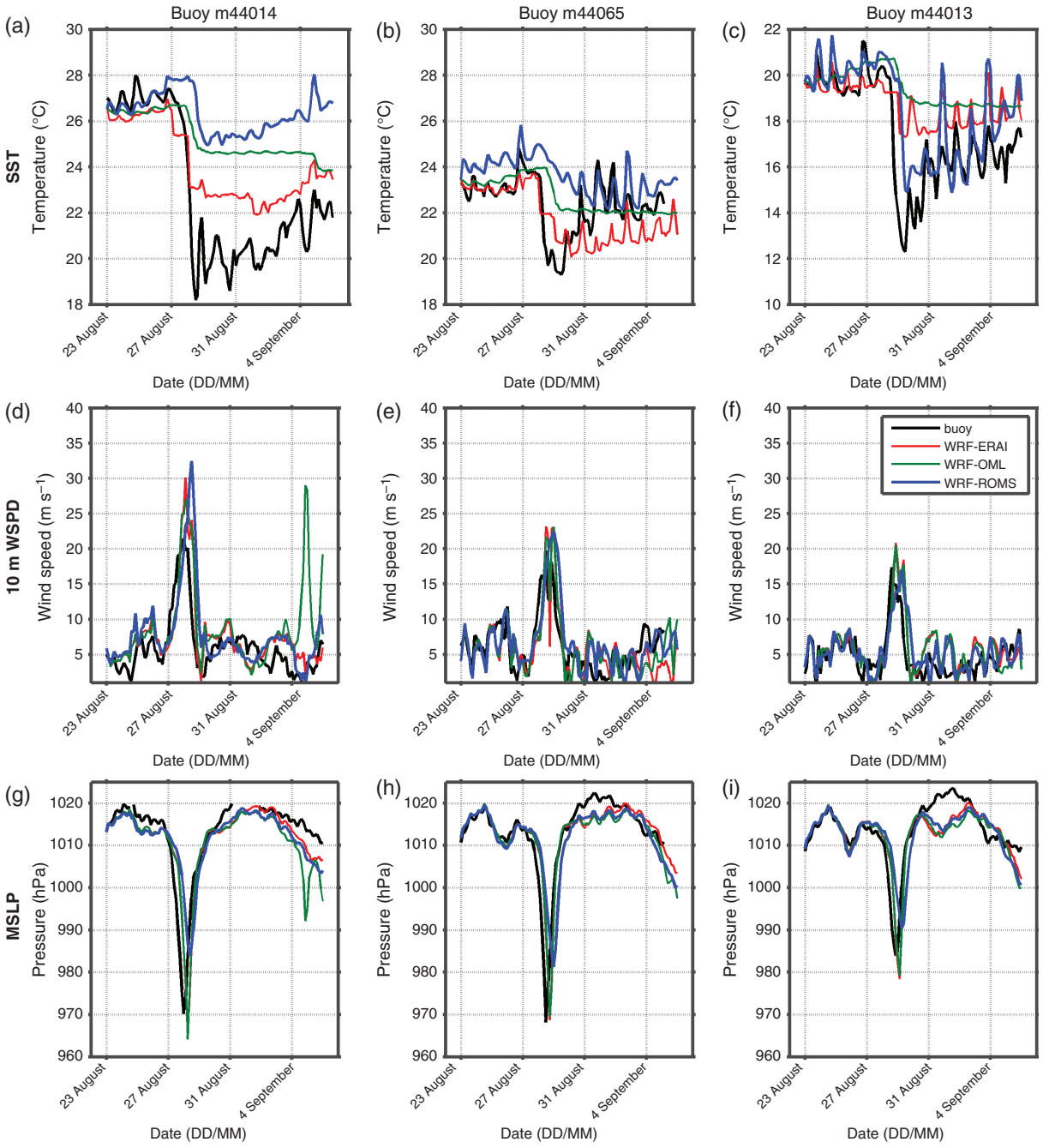

Figure 4. (a)–(c) Simulated and measured sea surface temperatures at buoys m44014, m44065 and m44013 covering the period 23 August 2011 to 6 September 2011. (d)–(f) Same as (a)–(c) except for 10-m wind speeds. (g)–(i) Same as (a)–(c) except for mean sea level pressure.

Recovery to climatological values is primarily driven by surface fluxes and horizontal advection (Vincent *et al.*, 2012). As the OML model does not include horizontal advection, it is foreseeable that its SSTs fail to recover to pre-storm conditions. While this suggests that the OML model is unsuitable for longer term studies, its computational efficiency and physically based representation of oceanic cooling make it an attractive option for future work. One approach which would retain computational efficiency will focus on representing the recovery of SSTs by adding a relaxation term based on empirical data.

Table 3. Root mean squared errors (RMSEs) for the tracks and intensity of hurricane Irene simulated by the three simulations listed in Table 1.

	WRF–ERAI	WRF–OML	WRF–ROMS
Tracks (km)	56	58	113
Intensity (hPa)	9	9	8

Acknowledgements

The authors are grateful to Dr. John Warner (USGS, Woods Hole) for providing access to the COAWST modelling system. NCAR is sponsored by the National Science Foundation

(NSF). This work was partially supported by NSF EASM Grant AGS-1048829 and the Research Partnership to Secure Energy for America. The authors acknowledge high-performance computing support from Yellowstone (ark:/85065/d7wd3xhc) provided by NCAR's Computational and Information Systems Laboratory, sponsored by the NSF. Part of the data analysis in this work was undertaken with climate data operators (CDO).

References

Balaguru K, Taraphdar S, Leung LR, Foltz GR, Knaff JA. 2014. Cyclone-cyclone interactions through the ocean pathway. *Geophysical Research Letters* **41**: 6855–6862, doi: 10.1002/2014GL061489.

de Boyer Montégut C, Madec G, Fischer AS, Lazar A, Iudicone D. 2004. Mixed layer depth over the global ocean: an examination of profile data and a profile-based climatology. *Journal of Geophysical Research* **109**: C12003, doi: 10.1029/2004JC002378.

Brand S. 1971. The effects on a tropical cyclone of cooler surface waters due to upwelling and mixing produced by a prior tropical cyclone. *Journal of Applied Meteorology* **10**(5): 865–874.

Bruyère CL, Holland GJ, Towler E. 2012. Investigating the use of a genesis potential index for Tropical Cyclones in the North Atlantic Basin. *Journal of Climate* **25**: 8611–8626, doi: 10.1175/JCLI-D-11-00619.1.

Chen F, Dudhia J. 2001. Coupling an advanced land surface-hydrology model with the Penn State-NCAR MM5 modeling system Part I: model implementation and sensitivity. *Monthly Weather Review* **129**: 569–585.

Collins WD, Rasch PJ, Boville BA, Hack JJ, McCaa JR, Williamson DL, Kiehl JT, Briegleb B, Bitz C, Lin S-J, Zhang M, Dai Y. 2004. Description of the NCAR Community Atmosphere Model (CAM3.0). NCAR Technical Note, TN-464+STR, NCAR, Boulder, CO, USA, 102–143.

Costa P, Gómez B, Venâncio A, Pérez E, Pérez-Munuzuri V. 2012. Using the Regional Ocean Modeling System (ROMS) to improve the sea surface temperature predictions of the MERCATOR Ocean System. In *Advances in Spanish Physical Oceanography*, Espino M, Font J, Pelegrí JL, Sánchez-Arcilla A (eds). Scientia Marina 76S1: Barcelona, Spain; 165–175. ISSN: 0214-8358; doi: 10.3989/scimar.03614.19E.

Cummings JA. 2005. Operational multivariate ocean data assimilation. *Quarterly Journal of the Royal Meteorological Society* **131**: 3583–3604, doi: 10.1256/qj.05.105.

Dare RA, McBride JL. 2011. Sea surface temperature response to tropical cyclones. *Monthly Weather Review* **139**(12): 3798–3808.

Davis CAW, Wang W, Chen SS, Chen Y, Corbosiero K, DeMaria M, Dudhia J, Holland G, Klemp J, Michalakes J, Reeves H, Rotunno R, Snyder C, Xiao Q. 2008. Prediction of landfalling hurricanes with the advanced hurricane WRF model. *Monthly Weather Review* **136**: 1990–2005, doi: 10.1175/2007MWR2085.1.

Dee DP, Uppala SM, Simmons AJ, Berrisford P, Poli P, Kobayashi S, Andrae U, Balmaseda MA, Balsamo G, Bauer P, Bechtold P, Beljaars ACM, van de Berg L, Bidlot J, Bormann N, Dlesol C, Dragani R, Fuentes M, Geer AJ, Haimberger L, Healy SB, Hersbach H, Hólm EV, Isaken L, Källberg P, Kohler M, Matricardi M, McNally AP, Monge-Sanz BM, Morcrette J-J, Park BK, Peubey C, de Rosnay P, Tavoloato C, Thépaut J-N, Vitart F. 2011. The ERA-Interim reanalysis: configuration and performance of the data assimilation system. *Quarterly Journal of the Royal Meteorological Society* **137**: 553–597, doi: 10.1002/qj.828.

Glenn SM, Miles TN, Seroka GN, Xu Y, Forney RK, Yu F, Roarty H, Schofield O, Kohut J. 2016. Stratified coastal ocean interactions with tropical cyclones. *Nature Communications* **7**: 10887, doi: 10.1038/ncomms10887.

Hart RE, Maue RN, Watson MC. 2007. Estimating local memory of tropical cyclones through MPI anomaly evolution. *Monthly Weather Review* **135**(12): 3990–4005.

Hong S-Y, Lim J-OJ. 2006. The WRF single moment six class scheme (WSM6). *Journal of the Korean Meteorological Society* **42**: 129–151.

Hong S-Y, Noh Y, Dudhia J. 2006. A new vertical diffusion package with an explicit treatment of entrainment processes. *Monthly Weather Review* **134**: 2318–2341.

Kain JS. 2004. The Kain-Fritsch convective parameterization: an update. *Journal of Applied Meteorology* **43**: 170–181.

Kain JS, Fritsch JM. 1990. A one-dimensional entraining/detraining plume model and its application in convective parameterization. *Journal of the Atmospheric Sciences* **47**: 2784–2802.

Knapp KR, Kruk MC, Levinson DH, Diamond HJ, Neumann CJ. 2010. The International Best Track Archive for Climate Stewardship (IBTrACS): unifying tropical cyclone data. *Bulletin of the American Meteorological Society* **91**: 363–376.

Leipper DF. 1967. Observed ocean conditions and Hurricane Hilda. *Journal of the Atmospheric Sciences* **24**: 182–196.

Lin I, Liu WT, Wu C-C, Wong GTF, Hu C, Chen Z, Liang W-D, Yang Y, Liu KK. 2003. New evidence for enhanced ocean primary production triggered by tropical cyclone. *Geophysical Research Letters* **30**: 1718, doi: 10.1029/2003GL017141.

Pollard RT, Rhines PB, Thompson RORY. 1972. The deepening of the wind-mixed layer. *Geophysical Fluid Dynamics* **4**(1): 381–404, doi: 10.1080/03091927208236105.

Price JF. 1981. Upper ocean response to a hurricane. *Journal of Physical Oceanography* **11**(2): 153–175.

Shchepetkin AF, McWilliams JC. 2005. The regional ocean modeling system: a split-explicit free-surface, topography-following coordinates ocean model. *Ocean Model* **9**: 347–404, doi: 10.1016/jocemod.2004.08.002.

Skamarock WC, Klemp JB, Dudhia J, Gill DO, Barker DM, Duda MG, Huang X-Y, Wang W, Powers JG. 2008. A description of the advanced research WRF Version 3. NCAR Technical Note, NCAR, Boulder, CO, USA.

Stark JD, Donlon CJ, Martin MJ, McCulloch ME. 2007. OSTIA: an operational, high resolution, real time, global sea surface temperature analysis system, Oceans 07 IEEE Aberdeen, conference proceedings. In *Marine Challenges: Coastline to Deep Sea*. IEEE: Aberdeen, Scotland.

Vincent EM, Lengaigue M, Madec G, Vialard J, Samson G, Jourdain NC, Menkes CE, Julien S. 2012. Processes setting the characteristics of sea surface cooling induced by tropical cyclones. *Journal of Geophysical Research* **117**: C02020, doi: 10.1029/2011JC007396.

Warner JC, Sherwood CR, Arango HG, Signell RP. 2005. Performance of four turbulence closure methods implemented using a generic length scale method. *Ocean Modelling* **8**: 81–113.

Warner JC, Armstrong B, He R, Zambon JB. 2010. Development of a Coupled Ocean–Atmosphere–Wave–Sediment Transport (COAWST) modeling system. *Ocean Modelling* **35**(3): 230–244.

Yablonsky RM, Ginis I, Thomas B, Tallapragada V, Sheinin D, Bernardet L. 2015. Description and analysis of the ocean component of NOAA's Operational Hurricane Weather Research and Forecasting Model (HWRF). *Journal of Atmospheric and Oceanic Technology* **32**(1): 144–163, doi: 10.1175/JTECH-D-14-00063.1.

Zeng X, Beljaars A. 2005. A prognostic scheme of sea surface skin temperature for modeling and data assimilation. *Geophysical Research Letters* **32**: L14605, doi: 10.1029/2005GL023030.